



Electron Density Estimation by Electrostatic Probe for Plasma Generated Near the Spacecraft Returning to the Earth's Atmosphere

Malak F. Hassan, Waleed I. Yaseen*

Department of Astronomy and Space, College of Science, University of Baghdad, Baghdad, Iraq

Received: 20/6/2022

Accepted: 4/9/2022

Published: 30/6/2023

Abstract

In this work, the electrostatic probe was utilized to estimate the density of electrons for plasma generated around reentry vehicles that have a geometrically blunt nose at high-altitude. The thermocouple uses to measured electron temperature, which is equal to the temperature of the gas, on board the MAC spacecraft. In the spacecraft backflow field, electrostatic probe measurements were taken at five separate regions 1 to 5 cm from the body of the spacecraft. Over an altitude range of 90 to 50 km with an electron density of 10^8 to 10^{12} $1/\text{cm}^3$, respectively. The measured electron temperature ranged from 0.05 to 0.9 electron volts and the maximum re-entry velocity of the spacecraft was about 7048 m/s in the re-entry experiment. The cooling using water jet in the flow field, the relationship between electron density, angle of attack changes, and the combustion products of the spacecraft's nose is also discussed.

Keywords Spacecraft Entry, Plasma diagnostics; Electrostatic probes, Electron Density

قياس كثافة الإلكترون بواسطة المسبار الكهروستاتيكي للبلازما المولدة بالقرب من المركبة الفضائية العائدة إلى الغلاف الجوي للأرض

ملاك فلاح، وليد إبراهيم*

قسم فضاء وفلك، كلية العلوم، جامعة بغداد، بغداد، العراق

الخلاصة

في هذا العمل، تم استخدام المسبار الكهروستاتيكي لقياس الكثافة الإلكترونية للبلازما المتولدة حول المركبات العائدة على ارتفاعات عالية والتي تحتوي على انف غير حاد هندسيًا. تم استخدام المزوج الحراري لقياس درجة حرارة الإلكترون، التي تساوي درجة حرارة الغاز، على متن المركبة الفضائية MAC. أجريت قياسات مسبار إلكتروستاتيكي في مجال التدفق العكسي للمركبة الفضائية في خمس نقاط منفصلة من 1 إلى 5 سم من سطح المركبة الفضائية. على مدى ارتفاع من 90 إلى 50 كم بكثافة إلكترون من 10^8 إلى 10^{12} / سم³، تراوحت درجة حرارة الإلكترون المقاسة من 0.05 إلى 0.9 إلكترون فولت وكانت أقصى سرعة عودة للمركبة الفضائية حوالي 7048 م / ث في تجربة العودة. كما تمت مناقشة التبريد باستخدام نفث

*Email: waleedib1972cnc@gmail.com

الماء في مجال التدفق والعلاقة بين كثافة الإلكترون ، وتغيرات زاوية الهجوم ، ونواتج الاحتراق لأنف المركبة الفضائية.

1. Introduction

Entry and re-entry mean finding special adverbs for the descent of the vehicle to the Earth, without effects on this vehicle during return. Re-entry means a vehicle who to pushes away from the surface of the Earth and returns a gain into the Earth. Entry means returning a vehicle into Earth's atmosphere from space or orbit. One of the most important problems of spaceflight is the safe return of the spacecraft with the payload to Earth. The stage re-entry vehicles on the Earth's surface is considered an important and dangerous stage of the space flight, and it needs large efforts to accomplish [1].

The presence of Earth's atmosphere is beneficial in that it serves to reduce the spacecraft's speed to a safe landing speed. The heating and deceleration associated with atmospheric reentry leads to serious design problems that could cause the spacecraft to burn and explode [2].

The strong shock waves on the front end of the vehicle cause the air to heat up severely during re-entry into the Earth's atmosphere, and this process results in the ionization, dissociation, and creation of relatively large quantities of electrons from atmospheric gases. Under such conditions, air can be considered as a chemically unbalanced gaseous mixture. Another important phenomenon that occurs on the surface of a spacecraft is called the catalytic phenomenon, and it is considered non-ideal behavior, where the recombination processes of the different types of gases in the flow are active, which increases heat transmission since more heat is produced during the synthesis of new molecular species [3]. One of the most crucial parts of the space journey is the re-entry phase. In order to prevent the spacecraft from exploding, its thermal and mechanical constraints must be respected when the spacecraft's kinetic energy is reduced into the atmosphere. Because the spacecraft is returning to Earth's atmosphere at a hypersonic speed, the high degree of enthalpy and intense heating might cause ionization processes in the air. Because of this, the spacecraft is surrounded by a layer of plasma composed of free electrons, ions and neutral gases. This plasma has a frequency that interacts with radio frequencies, leading to many effects, such as reflection, attenuation and refraction. As a result, communication between the spacecraft and the ground station is interrupted due to a lowered signal-to-noise ratio, in this case, the uplink and downlink of the data are down, and the correct communications between the spacecraft and the satellites are exposed to the GPS and the ground stations on the return trip [4]. Beginning with the first Mercury missions, several studies of communications blackout were conducted on return flights. Lennert and Rosenbaum [5] attempted to study the dimming in the Apollo mission, which required re-entry to the Moon. Air density and velocity were used to characterize these phenomena for a certain action frequency at the stagnation point. Techer [6] Dunn and Kang [7] as well as Evans et al. [8] have completed basic theoretical work. A few years later, correlating the findings with antenna locations using a degradation model gave the Spacecraft Radio Attenuation Measurements (RAM). The theoretical foundation was needed to examine the phenomena of communication fading during a series of supersonic return flights [9].

2. Calculations of cylindrical electrostatic probe

The ionic current was calculated and interpreted using the cylindrical electrostatic probe numerically by reference [10] above a wide range of densities and temperatures of electrons for constant plasmas that are also applicable to plasmas with flow parallel to the probe axis. Because it can be easily changed to accommodate for a random probe direction, this theory works best in the scenario of a flowing plasma. For the chosen values of the ratio from the sheath radius a to the probe radius R_p , the measured current varies together with the observed potential difference X_p between the probe and plasma. The measured current is calculated as the difference between the probe's collected current (I_+), and the random ion current (I_r).

Following are the probe area and the saturation ion current density given by:

$$I_r = \frac{n_e v_+}{4} (2\pi R_p L) \tag{1}$$

where n_e density of electrons, R_p probe radius, L length of probe and v_+ velocity of ions entering sheath. The velocity v_+ can be determine by:

$$v_+ = \sqrt{\frac{8kT_e}{\pi M}} \tag{2}$$

where k , T_e and M are Boltzmann's constant, electron temperature and ion mass respectively. The potential difference between the probe and the plasma (X_p) determine as:

$$X_p = \frac{e(V - V_\infty)}{kT_e} \tag{3}$$

where V probe potential V_∞ plasma potential. The ion sheath radius (a) can be determine as:

$$a = R_p + ds \tag{4}$$

ds indicate the thickness of the sheath and is given by:

$$ds = \lambda_D X_p^{3/4} \tag{5}$$

λ_D is called Debye length and is defined as [11]:

$$\lambda_D = \sqrt{\frac{\epsilon_0 kT_e}{e^2 n}} \tag{6}$$

where ϵ_0 is the permittivity of free space.

$$\Theta = \frac{L}{I_+ R_p} \left(V' + \frac{5kT_e}{e} \right)^{3/2} \left(1 + \frac{2.66}{\sqrt{X_p}} \right) \tag{7}$$

probe current (I_+) measured for absolute magnitude of applied probe bias V' can be write as:

$$I_+ = \gamma 2\pi R_p L j_i \tag{8}$$

where J_i is the ion saturation current density for a collisionless Maxwellian plasma at rest and is given by reference as [12]:

$$j_i = 0.4 n_e v_+ \tag{9}$$

The ion speed ratio S write as:

$$S = \frac{v_f}{v_+} \tag{10}$$

Where v_f is normal component of the flow velocity. The directed current is:

$$I_d = n_e v_f (2R_p L) = \rho v_f A \tag{11}$$

where ρ charge density A projected area of probe.

using simple orbital theory, the particles will be collected at radius r_a and can be get the radius by:

$$r_a = R_p \sqrt{\left(1 + \frac{V}{V_0} \right)} \tag{12}$$

$$R = \frac{I_n}{\sqrt{(1 + S^2)}} \tag{13}$$

$$H = \frac{X_p}{(1 + S^2)} \tag{14}$$

where R , and H are modified normalized probe current and ratio of modified potential energy to kinetic energy respectively. The positive ion density can be write as:

$$n = \frac{I_+}{\sqrt{(1 + S^2)} R \sqrt{\pi} e v_+ R_p L} \tag{15}$$

3. Experimental Part

Flight experiments of the spacecraft were conducted upon return to Earth at an average speed of 7048 m/s to obtain measurements of electrostatic sensors and thermocouples that are used to diagnose the plasma generated around the body of the spacecraft that has a convex front. The electrostatic probe, thermocouples, and fins of the spacecraft are described. There are two types of probe used in this study: electrostatic probe for measuring ionic currents and thermocouples for measuring gas temperature, which represents the electron temperature. The electrostatic probes consist of an iridium wire 0.0254 cm diameter and 0.5385 cm length at an angle of 45° sheathed with beryllium oxide, with respect to the plasma flow apparent beyond the leading edge of the beryllium oxide. Beryllium oxide is wedge-shaped and is found on both sides of the vehicle, one containing electrostatic probe and the other containing thermocouples. Iridium material was chosen as the collector of the probe due to its temperature of melting higher, high work function, and it is a non-oxidizing material. The advanced beryllium oxide material is a high-temperature insulator and is used to mechanically and electrically separate ion complexes and electron complexes. The leading edge of the beryllium oxide was a 60° wedge and was tilted at an angle of 45° with respect to the surface. Phenolic fiberglass is used to manufacture the probe's primary body. The thermocouples are placed opposite the electrostatic probe on the opposite side to monitor the temperature of the leading edge as shown in Figure 1. The locations of the probes and couplings in line with the cooling water injection process. The fin configurations of the thermocouples are the same as the fin configuration of the electrostatic probes, as shown in Figure 2. Three thermocouples were used from the leading edge of the fin. The thermocouples were made of platinum with 13% rhodium added and were located 2, 4 and 6 cm from the body of the spacecraft. The effective range for thermocouples was from -18.15 to 1703.85 Celsius, which correspond to 0.022 to 0.1704 eV.

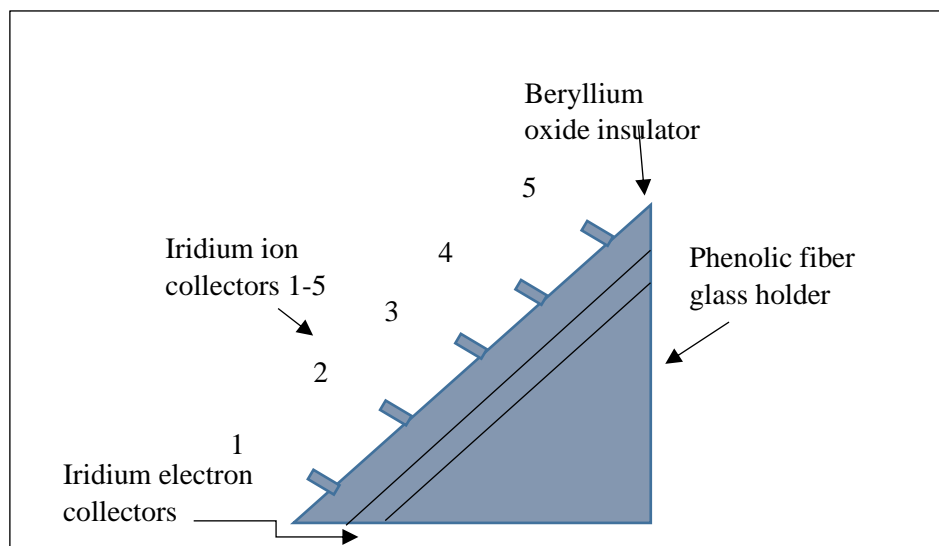


Figure 1: Configuration of the electrostatic probes

During the return flight, water was repeatedly jetted into the flow field from the spacecraft's convex front to obtain reductions in heat and electron density in the attenuation layer of the flow field. The water was jetted at varying flow rates over an altitude range from 90 to 50 km. The water jetting sites are shown in Figure 2.

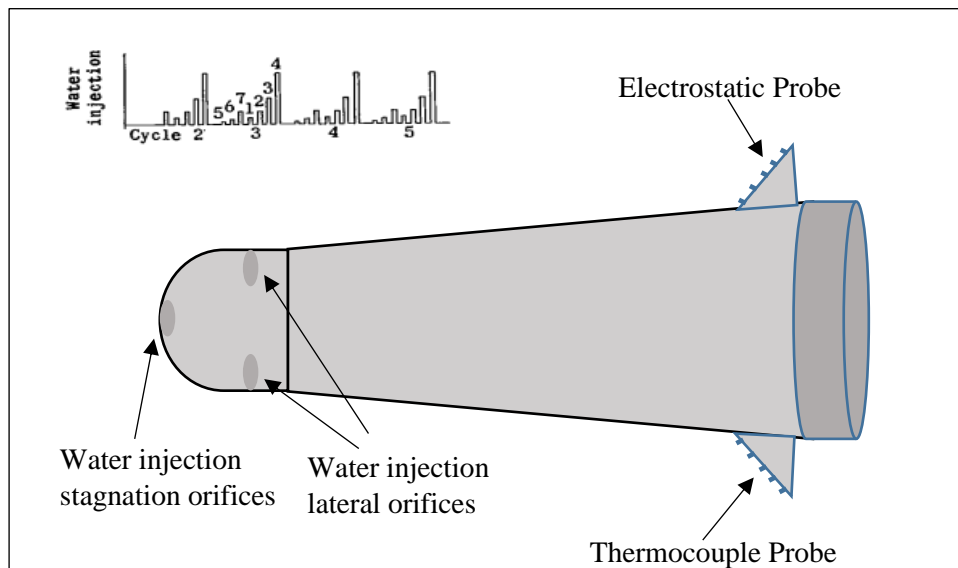


Figure 2: Configuration of RAM spacecraft.

The electrostatic probe was placed on the same line with the jetting places. Typical water flow pulsations are displayed as a sequence of valve operating times. The full jetting cycle is repeated every 5 seconds. Valves operating times were 250 msec and valves opened at 0.5 sec intervals as shown in Figure 2.

4. Results and Discussion

The ion currents that each of the five electrostatic probes are measured on the surface of the RAM spacecraft as a function of height from 90 to 50 km as shown in Figure 3. The initial current is measured by the probes at an altitude of 90 km was about 0.470 mA. The lowest current can be measured or the probe electronic system was about 10^{-7} A, also the system saturation current was 10^{-3} A. The currents taken by the electrostatic probes on board the spacecraft are shown in Figure 3. The effects of repeated jetting of water into the flow field can be observed as periods in which the measured currents decrease significantly for all five probes. The anomaly period occurred between 67.1 and 61.0 km. The period of the anomaly appears in these figures and depends on the operation of the logarithmic amplifier. The anomaly that occurs in the ionic current and electronic density data is caused by the amplifier stopping logarithmic that is used to process the data of the ionic current in the electrostatic probe circuit. The reason for stopping is due to the collecting of electrons near the body of the spacecraft, which results in a floating plasma that reduces the amplifier current to zero. This anomaly occurs at an altitude of 67.1 to 61 km.

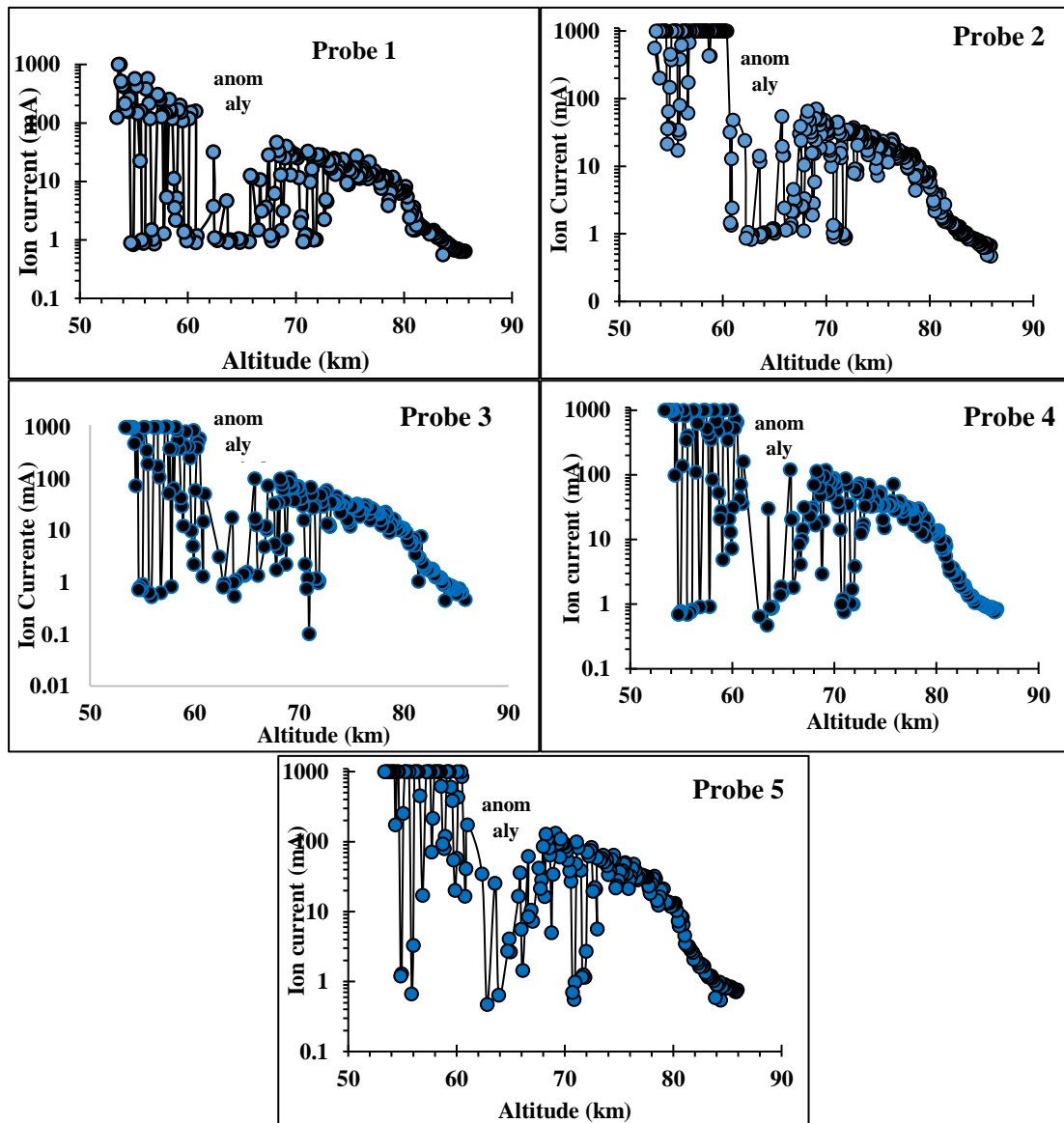


Figure 3: Ion currents by five electrostatic probes on the RAM flights.

Due to the electrical breakdown of the beryllium oxide probe dielectric caused by aerodynamic heating. The electrostatic probes measure the saturation current of the system. The small changes superimposed on the ionic current curves, shown in Figures 3, are changes that occur in the ionic current due to the movement of the spacecraft. The electron temperatures for the spacecraft RAM reentries are illustrated in Figure 4. Thermocouples corresponding to the electrostatic sensors at the same altitudes, measure lower temperatures due to the cooling effects of the repeated water jets. At 76.2 km altitude, the temperature calculated to be 0.6463 eV for the collector of ion 5. The local gas temperature is assumed to be equal to the electron temperature. Figure 5 illustrates the temperature of the gas as a function of time for the ion collector locations. These data of temperature, as well as the data of flow velocity given in Figures 6 and 7, generated by a flow-field analysis of the spacecraft trajectory.

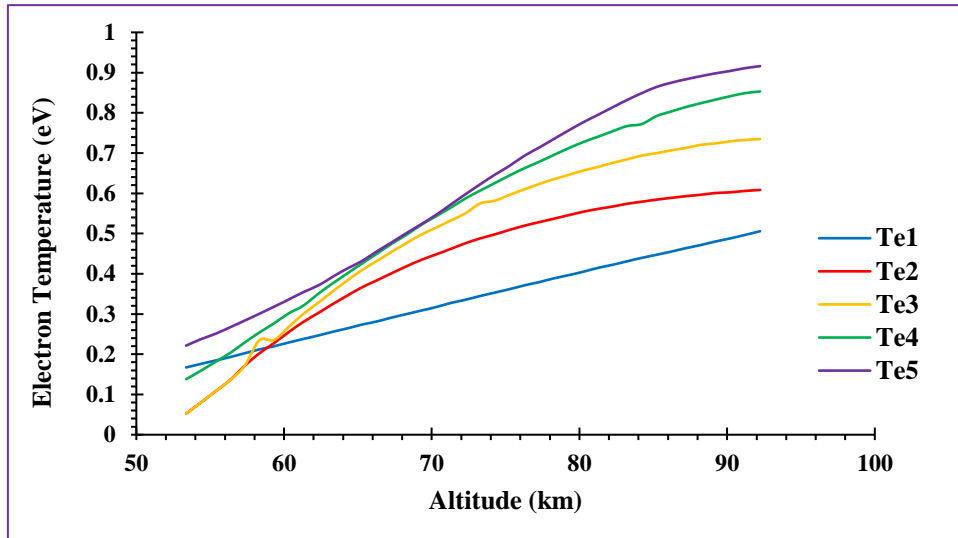


Figure 4: Thermocouple temperatures vs altitude for the RAM reentries

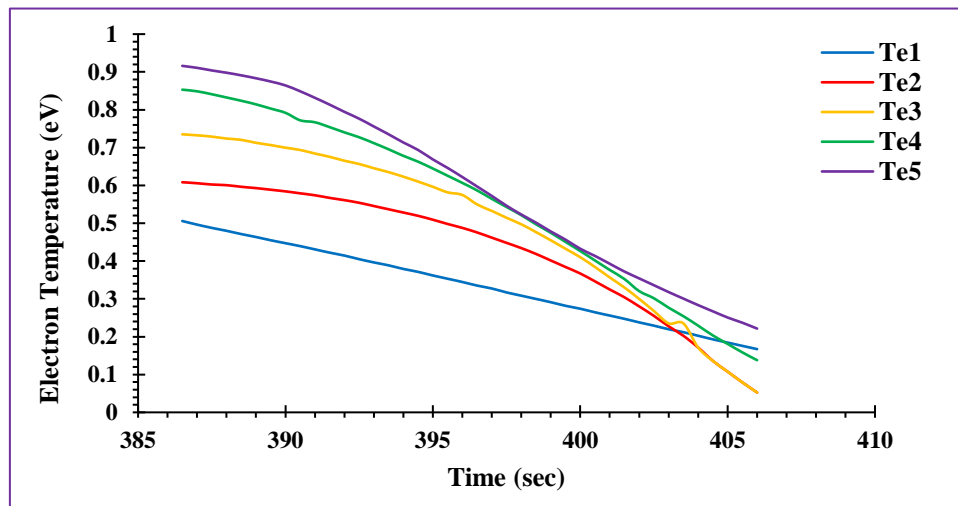


Figure 5: Thermocouple temperatures vs time for the RAM reentries

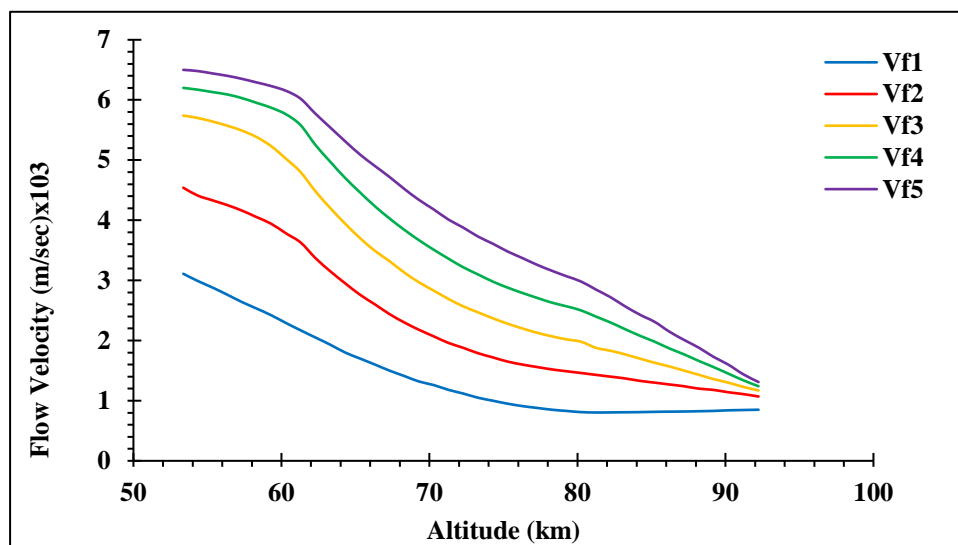


Figure 6: Flow velocity against with Altitude.

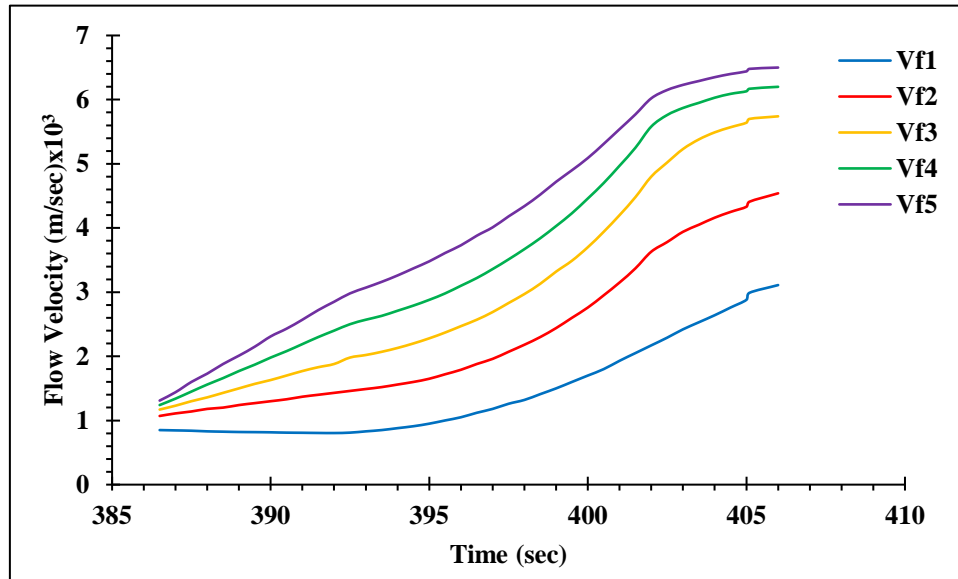


Figure 7: Flow velocity against with Time.

To calculate the electron density, the following steps are applied: first, calculate the potential difference between the plasma and the probes using Equation 3. Next, is the ratio of the probe radius to the ion sheath radius. (γ) is determined using a database in reference [13] and Equation 7. The normalized probe current R is now estimated by Equation 13 and H by Equation 14, the ion's velocity v_+ that enters the sheath is determined from Equation 2. Calculate the ion speed ratio S from Equation 10. The density n_e is solve using Equation 15. The ion or electron densities for the flight are calculated by using ion currents given in Figure 3. Figure 8 shows how flow-field calculations for the spacecraft's trajectory show that the positive-ion and electron densities are extremely close to being equal. The probe readings provide a great way to figure out how far the injectant penetrated as well as how much suppressed plasma created. The red circle in Figure 8 illustrates how much plasma repression from water injection has occurred on the spacecraft's plasma electron density. Every pulse results in commensurate reductions in the observed electron density. It is evident that increased flow rates have a greater impact on electron density reduction and allow them to penetrate further into the flow. Data analysis showed that the spacecraft experienced minute angle-of-attack oscillations that caused changes in the ion current measured by the five instruments indicated in Figure 9. Because the spacecraft was rotating at 20 rad/sec (3.18 RPS) while the flow field around it was asymmetrical, variations in electron density at the probes occurred.

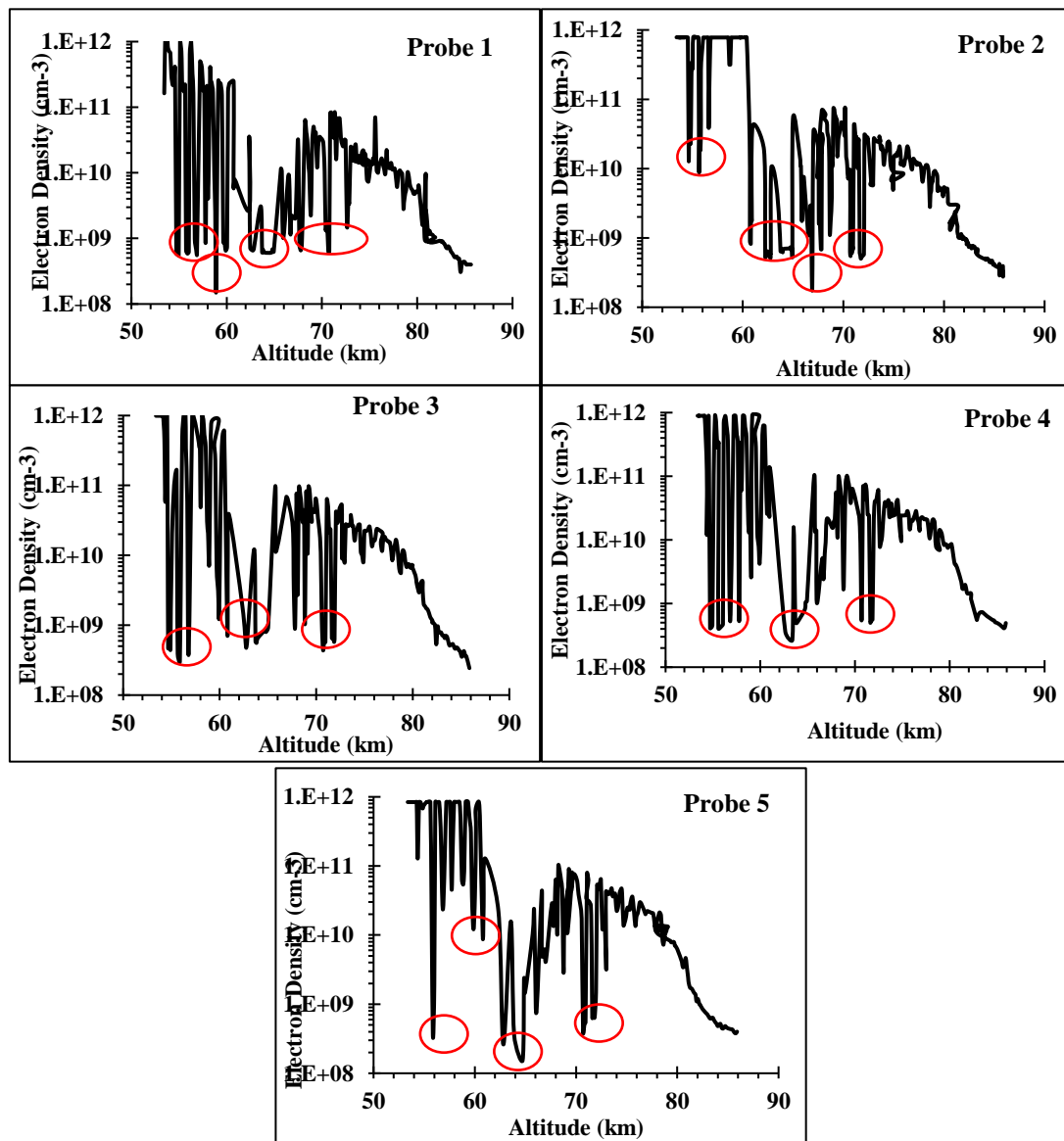


Figure 8: Electron densities for RAM spacecraft.

The electrostatic probes located on the windward side of the vehicle and measured the pressure of the flow field when the vehicle exposed to a positive angle of attack and positive normal acceleration. In contrast, as illustrated in Figure 10, the probes are sensing low density for a negative angle of attack at a normal negative acceleration.

The changes in the results of the measured electron densities presented due to the displacement of the electrostatic probe from the wind axis in the plane of the angle of attack (α). The differences produced peak-to-peak differences in densities in the angle of attack of $\alpha = -4^\circ$ and $+4^\circ$ for RAM spacecraft. The symmetry of the intensity difference indicates that the average values represent the state when $\alpha=0$.

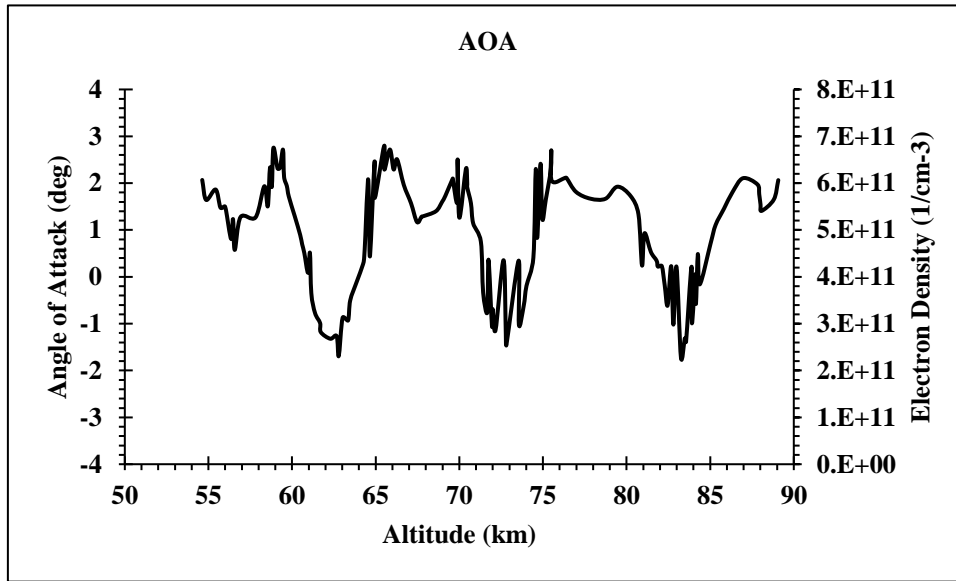


Figure 9: Effect of angle-of-attack on Electron density with altitude acceleration.

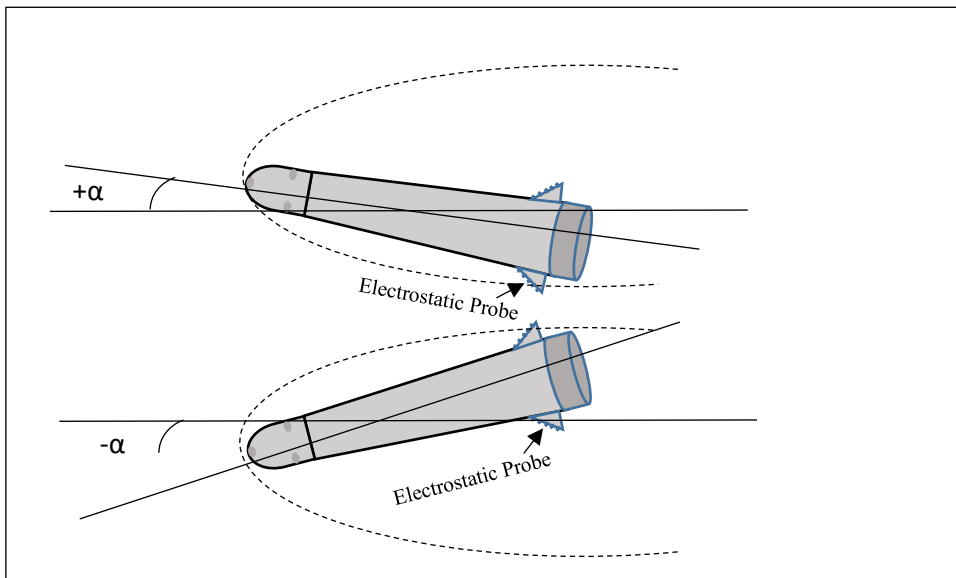


Figure 10: Angle-of-attack with positive and negative normal

Since the spacecraft nose material is combustible and charred, the plasma flow fields are contaminated with remnants of burnt nose material which affects the electron density calculations so that it is high for the altitude range of 86 to 74 km.

5. Conclusions

From the results of measurements of electrostatic probes and thermocouples that were made on the spacecraft entering the Earth's atmosphere at high speed, the following conclusions can be obtained:

Due to the combustion products of the spacecraft nose containing phenol-graphite in the backflow field, there was an increase in ionization when the spacecraft descended from a height of 90 to 50 km. Small changes in the angle of attack lead to fluctuations in electron density and is useful in determining the appropriate angle of attack for a re-entry spacecraft. Water added to the flow field has been shown to be effective in reducing electron density.

References

- [1] L. W.H., "*Reentry and Planetary Entry Physics and Technology*," Springer Science & Business Media New York Inc, 2013.
- [2] W. I. Yaseen, "Determination of Skip Entry Trajectories for Space Vehicles at Circular and Super Circular Speeds," *Iraqi Journal of Physics*, vol. 8, no. 12, pp. 29-34, 2010.
- [3] W. Grantham, "Flight Results of a 25000-Foot-Persecond Re-Entry Experiment Using Microwave Reflectometers to Measure Plasma Electron Density and Standoff Distance," NASA TN-D-6062, 1970.
- [4] R. Savino, M. E. D. Elia and a. V. Carandente, "Plasma Effect on Radiofrequency Communications for Lifting Reentry Vehicles," *Journal of Spacecraft and Rockets*, vol. 52, no. 2, pp. 1-9, 2015.
- [5] L. R. and B. and Rosenbaum, "Plasma Effects on Apollo Re-entry Communication," NASA TN-D-2732,, 1965.
- [6] T. F. J., "Attenuation in Re-Entry Communications," *Goddard Space Flight Center*, NASA, X-520-62-92, 1962.
- [7] M. G. a. K. S. Dunn, " "Theoretical and Experimental Studies of Reentry Plasmas," NASA CR-2232, 1973.
- [8] J. S. Evans, C. J. J. Shexnayder and P. W. and Hubert, "Boundary-Layer Profiles for a Entry of a Blunt Slender Body at High Altitude," NASA TN-D-7332, 1973.
- [9] L. Zhao, B. W. Bai, W. M. Bao and X. P. and Li, "Effects of Reentry Plasma Sheath on GPS Patch Antenna Polarization Property," *International Journal of Antennas and Propagation*, vol. 2013, pp. 1-8, 2013.
- [10] G. Hok, N. W. Spencer, A. Reifman and W. G. and DOW, " Dynamic Probe Measurements in the Ionosphere," *AFCRC TN-U.S. Air Force*, 1958.
- [11] A. A.-K. Hussain, K. A. Aadim and a. W. I. Yaseen, "Diagnostics of low-pressure capacitively coupled RF discharge argon plasma," *Iraqi Journal of Physics*, vol. 13, no. 27, pp. 76-82, 2015.
- [12] B. David., E. H. S. Burhop and H. S. W. and Massey, *The Use of Probes for Plasma Exploration in Strong Magnetic Fields. The Characteristics of Electrical Discharges in Magnetic Fields*, McGraw-Hill Book CO, 1949.
- [13] W. L. Jones, "Electrostatic-probe measurements of plasma parameters for two reentry flight experiments at 25000 feet per second," *National Aeronautics And Space Administration . Washington*, 1972.